

SPECTRALLY RESOLVED PURE ROTATIONAL LINES OF WATER IN PROTOPLANETARY DISKS

KLAUS M. PONTOPPIDAN¹, COLETTE SALYK^{1,2}, GEOFFREY A. BLAKE¹, AND HANS ULRICH KÄUFL³*Draft version September 17, 2010*

ABSTRACT

We present ground-based high resolution N-band spectra ($\Delta v = 15 \text{ km s}^{-1}$) of pure rotational lines of water vapor in two protoplanetary disks surrounding the pre-main sequence stars AS 205N and RNO 90, selected based on detections of rotational water lines by the Spitzer IRS. Using VISIR on the Very Large Telescope, we spectrally resolve individual lines and show that they have widths of $30\text{--}60 \text{ km s}^{-1}$, consistent with an origin in Keplerian disks at radii of $\sim 1 \text{ AU}$. The water lines have similar widths to those of the CO at $4.67 \text{ }\mu\text{m}$, indicating that the mid-infrared water lines trace similar radii. The rotational temperatures of the water are 540 and 600 K in the two disks, respectively. However, the lines ratios show evidence of non-LTE excitation, with low-excitation line fluxes being over-predicted by 2-dimensional disk LTE models. Due to the limited number of observed lines and the non-LTE line ratios, an accurate measure of the water ortho/para ratio is not available, but a best estimate for AS 205N is ortho/para = 4.5 ± 1.0 , apparently ruling out a low-temperature origin of the water. The spectra demonstrate that high resolution spectroscopy of rotational water lines is feasible from the ground, and further that ground-based high resolution spectroscopy is likely to significantly improve our understanding of the inner disk chemistry recently revealed by recent Spitzer observations.

Subject headings: astrochemistry — planetary systems: protoplanetary disks

1. INTRODUCTION

The study of the dynamics and chemistry of the inner ($R < 10 \text{ AU}$) regions of disks around young pre-main sequence stars is a field in rapid growth, to a large extent thanks to the availability of sensitive infrared instrumentation, including the InfraRed Spectrograph (IRS) on the Spitzer Space Telescope. The molecular gas at these radii plays a key role in the process of planet formation, not only as a necessary reservoir for the formation of gas giants, but also in the generation and eventual delivery of volatile molecular species to terrestrial planets.

Recent observations have demonstrated that the mid-infrared wavelength range in protoplanetary disks contains a forest of molecular emission lines, many of them due to pure rotational transitions of water vapor (Carr & Najita 2008; Salyk et al. 2008; Pascucci et al. 2009; Pontoppidan et al. 2010). While Carr et al. (2004) detected and spectrally resolved rovibrational water lines at $2.3 \text{ }\mu\text{m}$ and Salyk et al. (2008) at $3 \text{ }\mu\text{m}$ from protoplanetary disks, the observations of the mid-infrared pure rotational lines were all carried out at $R = \lambda/\Delta\lambda \leq 600$, resulting in unresolved and blended line spectra. The rovibrational $2\text{--}3 \text{ }\mu\text{m}$ lines have much higher excitation temperatures, and may not probe the same gas as the mid-infrared rotational lines. Further, they also suffer from significant line blending, making it difficult to study the details of the excitation structure. In this Letter, we demonstrate that high resolution spectroscopy of *pure rotational transitions* of water in the atmospheric N-band window is possible. The rotational water lines observable from the ground have excitation temperatures of 3000–

6000 K, directly comparable to those of the well-studied CO rovibrational lines in the $4.7 \text{ }\mu\text{m}$ fundamental band (Najita et al. 2003; Blake & Boogert 2004; Brittain et al. 2007; Pontoppidan et al. 2008; Salyk et al. 2009), allowing for more accurate relative abundance measurements. Further, the lines are well separated from one another and do not suffer from blending with other species.

In this Letter, we present high resolution ($R \sim 20\,000$) N-band spectra of AS 205N and RNO 90, disks known to have strong water vapor emission (Salyk et al. 2008; Pontoppidan et al. 2010), obtained using the Very Large Telescope Imager and Spectrometer for the mid-InfraRed (VISIR, Lagage et al. 2004). Both disks are likely part of the Ophiuchus star forming cloud at a distance of 120 pc (Loinard et al. 2008). With stellar luminosities of 4.0 and $3.5 L_{\odot}$ (Chen et al. 1995) and spectral types of K5 and G5, the central stars have likely masses close to $1 M_{\odot}$ (e.g., Siess et al. 1997; Salyk et al. 2008; Pontoppidan & Blake 2010). RNO 90 in particular, being a single star, may be a fairly close analog to the young Sun, while AS 205N is the primary of a 1'3 binary (160 AU).

2. OBSERVATIONS

Six water lines with excitation energies varying from 3300–5800 K were selected using the list of Pontoppidan et al. (2009) in combination with the limitations imposed by the availability of filters on VISIR. While telluric water generates highly pressure-broadened absorption, we find that even from a relatively low site, such as Paranal Observatory (2635 m), the atmospheric transmission for all our targeted lines is $>30\%$, and often significantly better.

Spectra centered on 12.405 and $12.454 \text{ }\mu\text{m}$ were observed using the cross-dispersed mode of VISIR, with a chop-throw of $8''$. In this mode, one source position is off the slit because the minimum chop-throw is larger than the slit length. Additional settings centered on 12.829 and $12.893 \text{ }\mu\text{m}$ were observed using the long-slit mode,

¹ California Institute of Technology, Division of Geological and Planetary Sciences, MS 150-21, Pasadena, CA 91125; pontoppi@gps.caltech.edu

² The University of Texas at Austin, Department of Astronomy, 1 University Station C1400, Austin, Texas 78712, USA

³ European Southern Observatory, Karl-Schwarzschild-Strasse 2, 85748 Garching bei Munchen, Germany

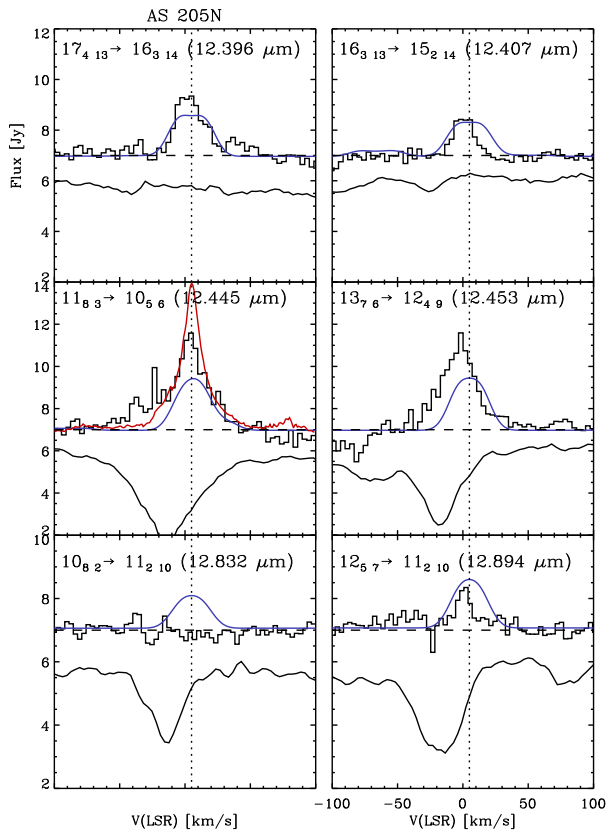


FIG. 1.— VISIR spectra of rotational water lines observed in AS 205N. The curves below the spectra show the standard star spectra, which are a combination of the spectral response function and the atmospheric transmission. The velocity range of the spectra is referenced to the local standard of rest. The red curve is the CO rovibrational ($\Delta v = 1$) line shape ($J < 8$), as observed with CRILES (Pontoppidan & Blake 2010), whose center defines the vertical dotted line. The blue curves are lines calculated using an LTE 2D disk model (see text for details).

in which all source positions are on slit, doubling the effective exposure time. The effective on source exposure times were 1250 s and 2500 s for the cross-dispersed and long-slit modes for AS 205N, respectively. For RNO 90, these exposure times were doubled. All observations were carried out using the $0''.75$ slit during good seeing conditions, specifically ensuring that components of the AS 205 binary are well separated. AS 205N was observed on August 5 and 6, 2009, while RNO 90 was observed on separate nights between August 9, 2009 and September 11, 2009. The spectral images were co-added using the ESO VISIR pipeline version 3.2.2. Chopping parallel to the slit removes most of the sky background, but a significant residual, especially from rapidly varying atmospheric water lines, is still visible. These residuals were removed by subtracting the median of each row (in the cross-dispersion direction) from the spectral image. The 1D spectra were generated using optimal extraction (Horne 1986). The wavelength calibration from the ESO pipeline was used, and is computed by cross correlating the sky emission spectrum with an atmospheric model generated using HITRAN (Rothman et al. 2005).

The spectral response function and atmospheric transmission spectrum were measured using observations of a bright infrared excess source known to not display strong water emission at $12\mu\text{m}$ in the survey of Pontoppidan

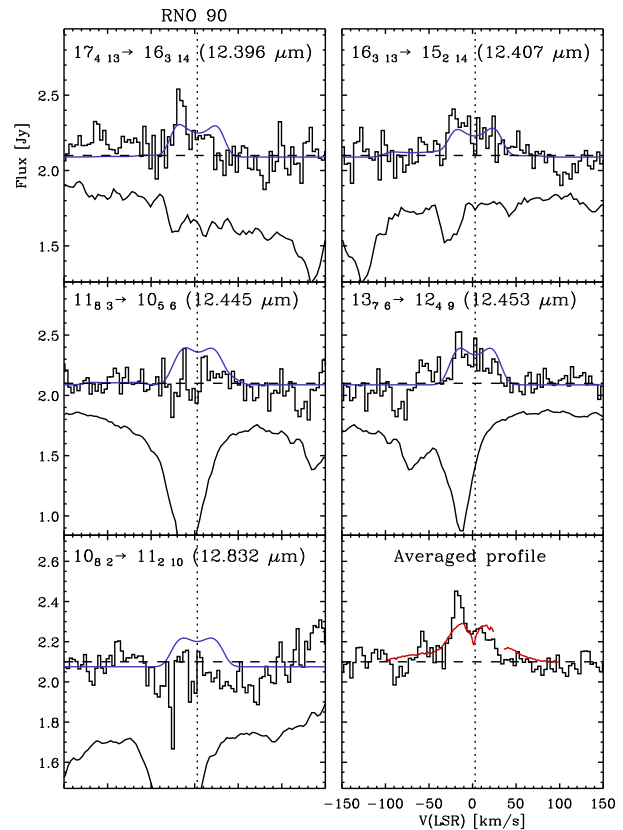


FIG. 2.— Same as Figure 1, but for RNO 90. The lower right panel presents the average of the three detected lines. The asymmetry visible as an increase in flux on the blue side of the detected lines is possibly real, but since it coincides with the telluric water lines, we are hesitant to discuss it in detail without further observations, preferably with different reflex motion doppler shifts.

et al. (2010), specifically the bright Herbig Ae/Be star HD150193. Ideally, a hot star without excess should be used, but no such source is sufficiently bright in the N-band. One could use a later type star, but in that case photospheric absorption lines will be present that may be difficult to remove. Hence, the choice was made to use an excess source dominated by continuum emission and with no apparent lines. Corrections for small shifts (of order a few pixels) between the source spectrum and that of the standard as well as a correction for differences in water column densities using a simple Lambert-Beer law were made to minimize the telluric residuals. The absolute fluxes were scaled to match those of the Spitzer spectra in Pontoppidan et al. (2010).

For comparison with the water lines, we use archival M-band high resolution ($R=100,000$) spectra of the CO rovibrational fundamental ($\Delta v = 1$) lines observed with CRILES. The CO lines have roughly the same upper level energies as the N-band rotational water lines. The CRILES data set will be described in greater detail in a spectro-astrometric survey (Pontoppidan & Blake 2010). It was processed following the procedures of Pontoppidan et al. (2008). Finally, we extracted an isolated lower energy line for comparison from the Pontoppidan et al. (2010) Spitzer spectra. The low-resolution ($R=600$) Spitzer spectra do not allow for the measurement of many unblended lines, but there are a few exceptions, one of them being the $10_4 7 \rightarrow 9_3 6$ ortho line at $33.5\mu\text{m}$.

TABLE 1
H₂O LINE FLUXES

Line	Wavel. μm	E_{upper} K	AS 205N ^a	RNO 90 ^a
17 ₄ 13 \rightarrow 16 ₃ 14 (o)	12.396	5746	4.8 ± 0.2	0.7 ± 0.08
16 ₃ 13 \rightarrow 15 ₂ 14 (p)	12.407	4915	2.3 ± 0.2	0.9 ± 0.11
13 ₇ 6 \rightarrow 12 ₄ 9 (o)	12.453	4187	10.4 ± 0.2	1.0 ± 0.14
11 ₈ 3 \rightarrow 10 ₅ 6 (o)	12.445	3606	11.4 ± 0.3	< 0.3
12 ₅ 7 \rightarrow 11 ₂ 10 (p)	12.893	3290	1.9 ± 0.2	< 0.3
10 ₈ 2 \rightarrow 9 ₅ 5 (p)	12.832	3223	< 0.4	< 0.2
10 ₄ 7 \rightarrow 9 ₃ 6 (o)	33.501	2260	1.9 ± 0.2	< 0.3

^a 10^{-14} erg cm⁻² s⁻¹

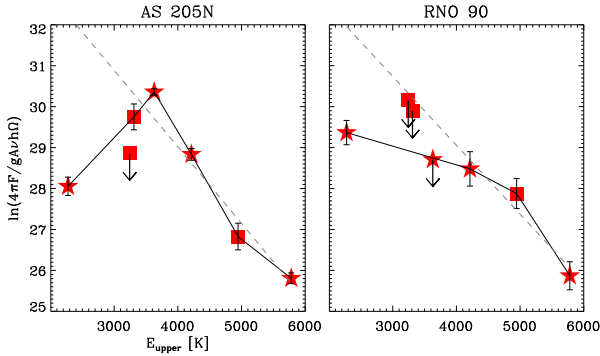


FIG. 3.— Rotation diagram for AS 205N and RNO 90. The star symbols are ortho lines, while the square symbols indicate para lines. The points include a spin degeneracy of 3:1. The dashed lines are the best fit single temperature models (using the detected VISIR lines only). The units are cgs and the symbols have their usual meaning.

3. RESULTS

The reduced VISIR spectra of AS 205N and RNO 90 are shown in Figures 1 and 2, respectively. For AS 205N, we detect 5 out of the 6 targeted lines, while 3 lines are detected for RNO 90. Integrated line fluxes are given in Table 1.

The lines, where detected, are spectrally resolved, with line widths of ~ 30 km s⁻¹ for AS 205N and ~ 60 km s⁻¹ for RNO 90. In the figures, the water lines are compared to the CO $\Delta v=1$ line shape. While variations are apparent for AS 205N, these differences are relatively minor, with FWHM of 20-35 km s⁻¹. similar to, or slightly less than those of CO. This indicates that the water lines are formed at similar or slightly larger disk radii. The high energy lines (17₄ 3 \rightarrow 16₃ 14, 16₃ 13 \rightarrow 15₂ 14) of AS 205N show indications of being flat-topped, while the lower excitation lines are single peaked, as is CO. All three detected RNO 90 lines are consistent with being double peaked, also matching the corresponding CO lines. The double peak is apparent when the three detected line profiles are averaged. We interpret this as evidence for a line origin in a Keplerian disk.

In order to estimate the properties of the emitting gas (rotational temperatures, radial distribution, column densities and abundances), we model the spectra using the 2D raytracer RADLite (Pontoppidan et al. 2009). We also construct rotation diagrams (Figure 3), which are designed to allow for easy comparison with a model consisting of a single-temperature slab of gas, and enable a discussion of the excitation and column density,

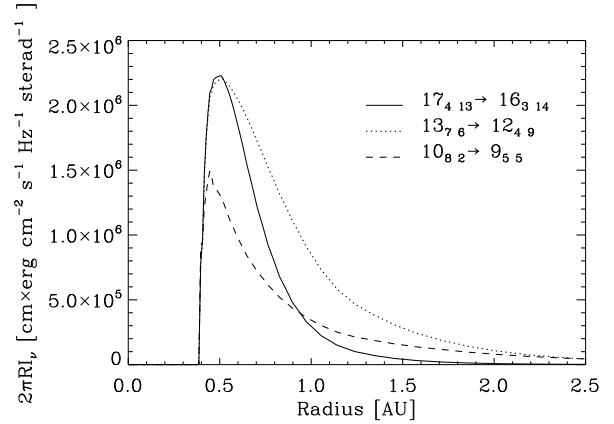


FIG. 4.— Continuum-subtracted surface brightness profiles of three lines for the RNO 90 model.

in an average sense, of the observed species; LTE level populations and optically thin emission predicts that line fluxes arrange along a straight line in the rotation diagram. Here we demonstrate that there are departures from the basic slab model assumptions of LTE, and that the assumption that all lines are formed in the same solid angle does not hold for water. Specifically, the slab model predicts significantly brighter 10₈ 2 \rightarrow 9₅ 5 and 12₅ 7 \rightarrow 11₂ 10 emission, by at least factors of 5-10, than what is observed for AS 205N. The upper limits on the RNO 90 lines are not strongly constraining, and the rotation diagram for this disk is roughly consistent with the slab model in the N-band, while the Spitzer 33.5 μm line is underluminous. The lower energy Spitzer line thus confirms the N-band turnover at lower energies in the rotation diagram for AS 205N. We stress that these are differences that are not apparent from the low-resolution Spitzer spectra alone. A linear regression of the VISIR lines on the linear part of the rotation diagram ($E_{\text{upper}} > 3500$ K) yields rotational temperatures of 540 and 600 K for AS 205N and RNO 90, respectively, for optically thin emission.

The AS 205N temperature can be compared to the 1000 K required to fit the 3 μm rovibrational lines (Salyk et al. 2008), indicating that the rotational lines indeed trace cooler gas. The selection of lines includes ortho- and para-transitions. The assumption that the N-band lines should form a straight line in the rotation diagram allows an estimate to be made of the ortho/para ratio. The paucity of lines, and the presence of clear departures from LTE and/or slab geometry unfortunately makes such an estimate uncertain. Nevertheless, scaling the three ortho-lines for AS 205N with energies between 3500 and 6000 K to an optimal alignment with the two detected para lines results in an apparent O/P ratio of 4.5 ± 1.0 for AS 205N. The ratio is higher than 3 because the para lines are placed below a straight line defined by the three ortho lines, but by less than 2σ . While this measurement is certainly affected by the caveats discussed above, we interpret this as indicative of a warm gas-phase (equilibrium) chemistry, as opposed to water formed in a low-temperature environment (< 60 K) via grain-surface chemistry, which would produce O/P ratios < 3 . Indeed, cometary water has O/P ratios corresponding to spin temperatures of ~ 30 K (Crovisier et al. 1997; Kawakita et al. 2004), and optical depth effects would

drive the estimated O/P values lower.

Since the lines are now spectrally resolved, the emitting area and hence the column density of the emitting gas can be directly estimated by converting the line width to a physical location in a Keplerian disk. The inclination of the RNO 90 disk is $\sim 45^\circ$ (Pontoppidan & Blake 2010) and the star has a mass of $\sim 0.9 M_\odot$ (Andrews et al. 2009). The RNO 90 water lines extend to $\sim 30 \text{ km s}^{-1}$, corresponding to an inner water line emitting radius of 0.45 AU. Similarly, for AS 205N the line width at zero flux corresponds to an inner emitting radius of 0.1-0.4 AU, for the $11_8 3 \rightarrow 10_5 6$ and $17_4 13 \rightarrow 16_3 14$ lines, respectively, assuming Keplerian flow, a disk inclination of 25° and a stellar mass of $1 M_\odot$ (Andrews et al. 2009). The effective outer radii of the emitting areas are determined by generating 2D models for the lines with RADLite, assuming LTE level populations. The model uses a simple parametrized flared disk structure (Dullemond et al. 2001), with inner radii fixed according to the observed line widths. The water abundance is set to 2.6×10^{-4} per H and the disk surface gas-to-dust ratio set to 1.28×10^4 , simulating significant dust settling, as discussed in Meijerink et al. (2009). Finally, the stellar luminosities were adjusted to match the dust continuum at $12.5 \mu\text{m}$. The resulting line strengths and profiles match well to those of the detected N-band lines with $E > 4000 \text{ K}$, as was already suggested by the rotation diagram (see Figures 1 and 2). Figure 4 shows the corresponding line surface brightness from the RADLite model, demonstrating that the RNO 90 emission is dominated by radii from 0.4 to 1.0 AU ($\sim 2.6 \text{ AU}^2$), but with the emitting area changing by a factor 2-3, depending on the line. Due to the higher luminosity of AS 205N, emitting radii span a wider range, here from 0.35 to 2.5 AU ($\sim 19 \text{ AU}^2$). Using these measures, the column densities of water, averaged over the emitting radii, are 2×10^{18} and $3 \times 10^{18} \text{ cm}^{-2}$.

4. DISCUSSION

We have detected pure rotational lines from water vapor (H_2^{16}O) in protoplanetary disks around T Tauri stars from the ground using transitions in the atmospheric N-band window. Gas temperatures of 500-600 K are found, while the line widths of $30\text{-}60 \text{ km s}^{-1}$ confirm that the disk surface at radii of 0.4-2.5 AU is forming the lines. The resolved lines enable a much more direct determination of the emitting area and hence the column density of the water, as compared to that possible for spectrally unresolved Spitzer observations. We find that the assumptions used for the analysis of the Spitzer data generally hold, i.e. that the lines are formed in the surface of Keplerian disks at radii of $\sim 1 \text{ AU}$. The water column densities are found to be a little higher for AS 205N than those determined by Salyk et al. (2008) using rotational lines at somewhat longer wavelengths

and lower energies. This appears to be consistent with the rotation diagram that indicates that lower excitation lines are less bright than expected for LTE level populations. This effect was also noted by Meijerink et al. (2009), who interpreted it as a depletion of water beyond $\sim 1 \text{ AU}$. More extensive N-band studies will help to further constrain the shape of the water rotation diagram to constrain the excitation and spatial distribution of water vapor in the inner regions of protoplanetary disks.

The derived water abundance is close to that predicted by Bethell & Bergin (2009), based on a chemical model that includes water self-shielding. The 2D RADLite models of both disks require high water abundances and high gas-to-dust ratios in order to reproduce the observed lines – a significant fraction of the available oxygen must be locked up in water vapor, and substantial dust settling to the disk midplane appears to have already taken place. An initial estimate of the ortho/para ratio of the water suggests a value consistent with a high temperature equilibrium (O/P=3), but higher signal-to-noise observations of more lines is required to confirm a high O/P ratio. If confirmed, this is indicative of water formed via hot gas-phase chemistry, as opposed to water initially formed as ice in the outer disk and transported inwards as part of migrating solids.

The spectra demonstrate that it is possible to obtain high resolution spectra of individual rotational lines of water in protoplanetary disks from the ground, in spite of telluric water absorption. These new tracers of the warm molecular layer have several unique advantages: The excitation energies and collisional rates of the high rotational levels are very similar to those of the ubiquitous fundamental ro-vibrational band of CO at $4.7 \mu\text{m}$. Given the chemical stability of CO, this allows for detailed studies of the relative water abundances in a well-defined location in the disk surface. The lines are strong, also relative to the continuum, and their analysis is not hampered by strong photospheric lines from the central star – in contrast to the weaker, much higher energy water lines in the $3 \mu\text{m}$ “hot band” (Salyk et al. 2008). The N-band lines may provide our only opportunity to obtain detailed velocity information of water at $\sim 1\text{--}10 \text{ AU}$ in disks around young solar analogs for the foreseeable future. Their observability from the ground also make them available to the very high spatial resolution line imaging of 10m class telescopes, as well as the next generation of Extremely Large Telescopes. As such, they will be important complements to the lower resolution spectroscopy of the James Webb Space Telescope.

Based on observations made at the ESO Paranal Observatory under program IDs 084.C-0635 and 179.C-0151. The authors acknowledge valuable discussions with Alain Smette.

REFERENCES

- Andrews, S. M., Wilner, D. J., Hughes, A. M., Qi, C., & Dullemond, C. P. 2009, *ApJ*, 700, 1502
 Bethell, T., & Bergin, E. 2009, *Science*, 326, 1675
 Blake, G. A., & Boogert, A. C. A. 2004, *ApJ*, 606, L73
 Brittain, S. D., Simon, T., Najita, J. R., & Rettig, T. W. 2007, *ApJ*, 659, 685
 Carr, J. S., & Najita, J. R. 2008, *Science*, 319, 1504
 Carr, J. S., Tokunaga, A. T., & Najita, J. 2004, *ApJ*, 603, 213
 Chen, H., Myers, P. C., Ladd, E. F., & Wood, D. O. S. 1995, *ApJ*, 445, 377
 Crovisier, J., Leech, K., Bockelee-Morvan, D., Brooke, T. Y., Hanner, M. S., Altieri, B., Keller, H. U., & Lellouch, E. 1997, *Science*, 275, 1904
 Dullemond, C. P., Dominik, C., & Natta, A. 2001, *ApJ*, 560, 957
 Horne, K. 1986, *PASP*, 98, 609

- Kawakita, H., Watanabe, J., Furusho, R., Fuse, T., Capria, M. T., De Sanctis, M. C., & Cremonese, G. 2004, *ApJ*, 601, 1152
- Lagage, P. O. et al. 2004, *The Messenger*, 117, 12
- Loinard, L., Torres, R. M., Mioduszewski, A. J., & Rodríguez, L. F. 2008, *ApJ*, 675, L29
- Meijerink, R., Pontoppidan, K. M., Blake, G. A., Poelman, D. R., & Dullemond, C. P. 2009, *ApJ*, 704, 1471
- Najita, J., Carr, J. S., & Mathieu, R. D. 2003, *ApJ*, 589, 931
- Pascucci, I., Apai, D., Luhman, K., Henning, T., Bouwman, J., Meyer, M. R., Lahuis, F., & Natta, A. 2009, *ApJ*, 696, 143
- Pontoppidan, K. M., & Blake, G. A. 2010, *ApJ*, in prep
- Pontoppidan, K. M., Blake, G. A., van Dishoeck, E. F., Smette, A., Ireland, M. J., & Brown, J. 2008, *ApJ*, 684, 1323
- Pontoppidan, K. M., Meijerink, R., Dullemond, C. P., & Blake, G. A. 2009, *ApJ*, 704, 1482
- Pontoppidan, K. M., Salyk, C., Blake, G. A., Meijerink, R., Carr, J. S., & Najita, J. 2010, *ArXiv e-prints*
- Rothman, L. S. et al. 2005, *Journal of Quantitative Spectroscopy and Radiative Transfer*, 96, 139
- Salyk, C., Blake, G. A., Boogert, A. C. A., & Brown, J. M. 2009, *ApJ*, 699, 330
- Salyk, C., Pontoppidan, K. M., Blake, G. A., Lahuis, F., van Dishoeck, E. F., & Evans, II, N. J. 2008, *ApJ*, 676, L49
- Siess, L., Forestini, M., & Bertout, C. 1997, *A&A*, 326, 1001

